

Supporting Information

Molecular Engineering of Benzothiadiazole-Based Polymers: Balancing Charge Transport and Stretchability in Organic Field-Effect Transistors

Michael U. Ocheje,^{1§} Marc Comí,^{2§} Rui Yang,³ Zhihui Chen,³ Yao Liu,³ Nastaran Yousefi,¹ Mohammed Al-Hashimi,² Simon Rondeau-Gagné*¹*

¹ Department of Chemistry and Biochemistry, Advanced Materials Centre of Research, University of Windsor, Windsor, ON, Canada N9B 3P4.

² Department of Chemistry, Texas A&M University at Qatar, Education City, Doha, P.O. Box 23874, Qatar.

³ Beijing Advanced Innovation Center for Soft Matter, Science and Engineering, State Key Laboratory of Chemical Resource Engineering, Beijing University of Chemical Technology, Beijing, 100029, China

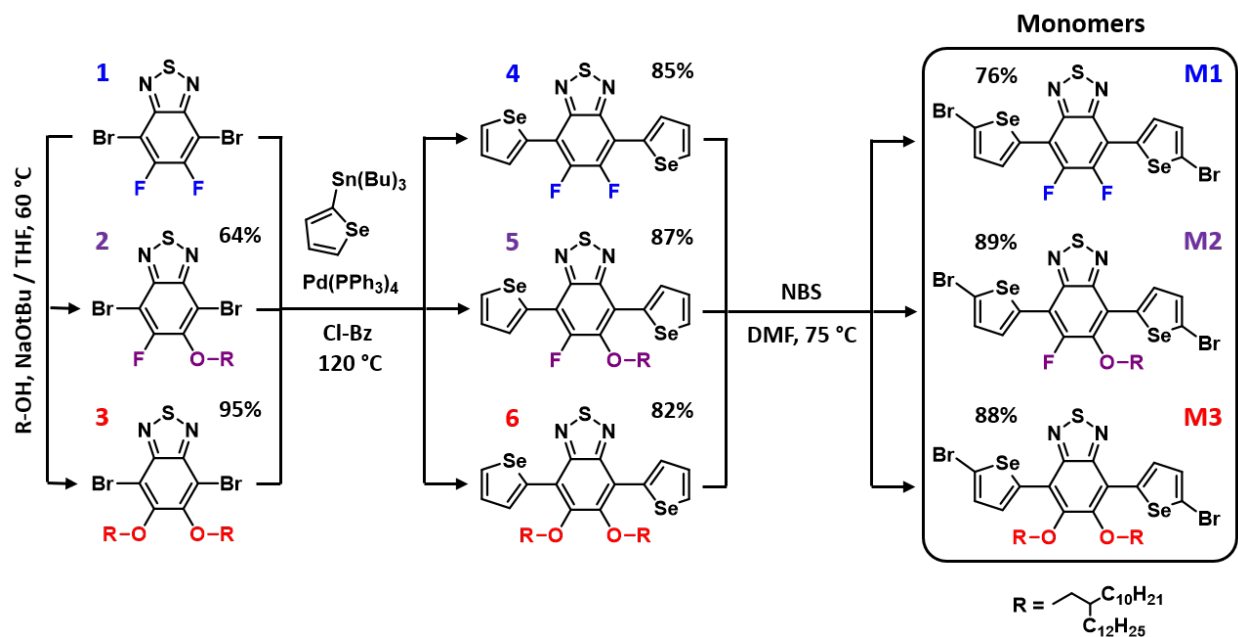
Table of contents:

- Materials and Methods
- Experimental Procedures
- NMR Characterization

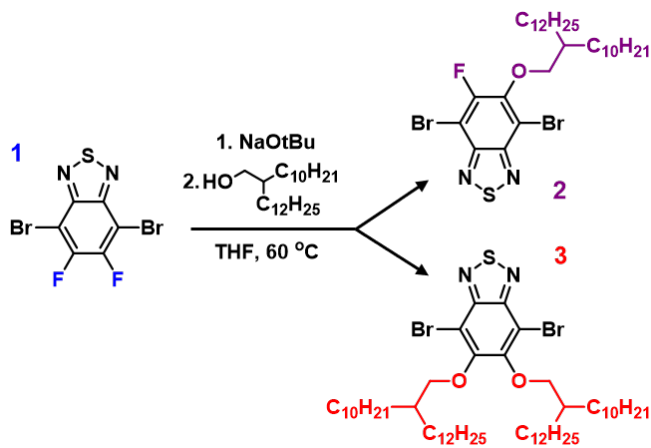
Materials and Methods

All commercially available solvents, reagents, and chemicals were used as received without further purification unless otherwise stated. Experimental procedure for the preparation of **M1** to **M3** was adapted from previous reports.^{1,2} Anhydrous solvent tetrahydrofuran was distilled from sodium under argon. 4,7-dibromo-5,6-difluorobenzo[*c*][1,2,5]thiadiazole, 2-decyltetradecan-1-ol, sodium tert-butoxide, *N*-bromosuccinimide were purchased from Sigma Aldrich. Unless otherwise stated, all operations and reactions were carried out under argon using standard Schlenk line techniques. ¹H, ¹⁹F and ¹³C NMR spectra were recorded on a Bruker AV-400 (400 MHz), using the residual solvent resonance of CDCl₃ or TMS as an internal reference and are given in ppm. Number-average (M_n) and weight average (M_w) were determined by Agilent Technologies 1200 series GPC running in chlorobenzene at 85 °C, using two PL mixed B columns in series, and calibrated against narrow polydispersity polystyrene standards. UV-vis spectra were recorded on a UV- 1601 Shimadzu Uv-vis spectrometer. Flash chromatography (FC) was performed on silica gel (Merck Kieselgel 60 F254 230-400 mesh) unless otherwise indicated. Thin Layer Chromatography (TLC) was performed on Merck aluminum-backed plates pre-coated with silica (0.2 mm, 60 F254). Microwave experiments were performed in a Biotage initiator V 2.3. Cyclic voltammetry (CV) measurements of polymers films were performed under argon atmosphere using a CHI760E Voltammetry analyzer with 0.1 M tetra-*n*-butylammonium hexafluorophosphate in acetonitrile as the supporting electrolyte. A platinum disk working electrode, a platinum wire counter electrode, and a silver wire reference electrode were employed, and the ferrocene/ferrocenium (Fc/Fc⁺) was used as the internal reference for all measurements. The scanning rate was 100 mV/s. Polymer films were drop-casted from chlorobenzene solutions on a Pt working electrode (2 mm in diameter). Doped wafers used for transfer-printing and device testing were purchased from University Wafer. The surface structure of polymer film was obtained using a Multimode atomic force microscope (AFM, Digital Instruments) operated in the tapping mode at room temperature. Images were collected using Nanoscope 6 software and processed using Gwyddion software.

Experimental Procedure



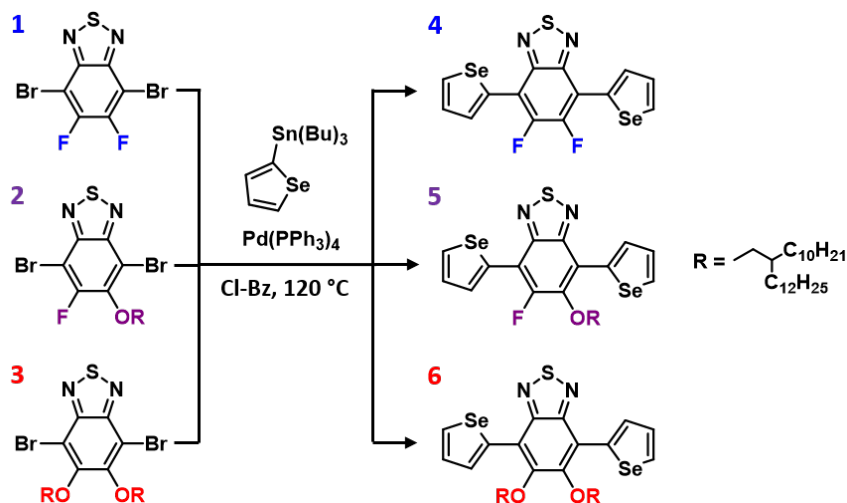
4,7-dibromo-5-((2-decyltetradecyl)oxy)-6-fluorobenzo[*c*][1,2,5]thiadiazole (**2**) and 4,7-dibromo-5,6-bis((2-decyltetradecyl)oxy)benzo[*c*][1,2,5]thiadiazole (**3**):



To a solution of 4,7-dibromo-5,6-difluorobenzo[*c*][1,2,5]thiadiazole **1** (5.00 g, 15.2 mmol) and 2-decyltetradecan-1-ol (5.37 g, 15.2 mmol or 10.74 g, 30.3 mmol) in anhydrous THF (100 mL) at r.t. was added sodium tert-butoxide (1.74 g, 18.2 mmol or 3.50 g, 36.4 mmol). After the addition, the reaction mixture was vigorously stirred at $60\text{ }^{\circ}\text{C}$ for 12 h. The solution was extracted with DCM (3 x 200 mL), the organic phase was dried and the solvent was removed under reduced

pressure, the crude product was purified by chromatography column using hexane to afford compound **2** as a white solid (6.45 g, 64%) or compound **3** as transparent syrup (13.38 g, 95%). Compound **2**. ^1H NMR (400 MHz, CDCl_3) δ 4.15 (d, $J = 6.4$ Hz, 2H), 1.88 (m, 1H), 1.63 (m, 2H), 1.22-1.55 (m, 38H), 0.90 (t, $J = 6.7$ Hz, 6H). ^{19}F NMR (376 MHz, CDCl_3) δ 119.6. ^{13}C NMR (100 MHz, CDCl_3) δ 158.0, 155.4, 150.0, 149.0, 98.7, 98.5, 78.2, 39.1, 31.9, 31.0, 30.0, 29.4, 26.8, 22.7, 14.1. Compound **3**. ^1H NMR (400 MHz, CDCl_3) δ 4.01 (d, $J = 6.4$ Hz, 4H), 1.92 (m, 2H), 1.58 (m, 4H), 1.22-1.50 (m, 76H), 0.89 (t, $J = 6.7$ Hz, 12H). ^{13}C NMR (100 MHz, CDCl_3) δ 154.8, 150.4, 106.0, 78.4, 39.2, 32.0, 31.3, 31.1, 30.0, 29.9, 29.8, 29.7, 29.6, 29.4, 26.9, 26.7, 22.7, 14.1.

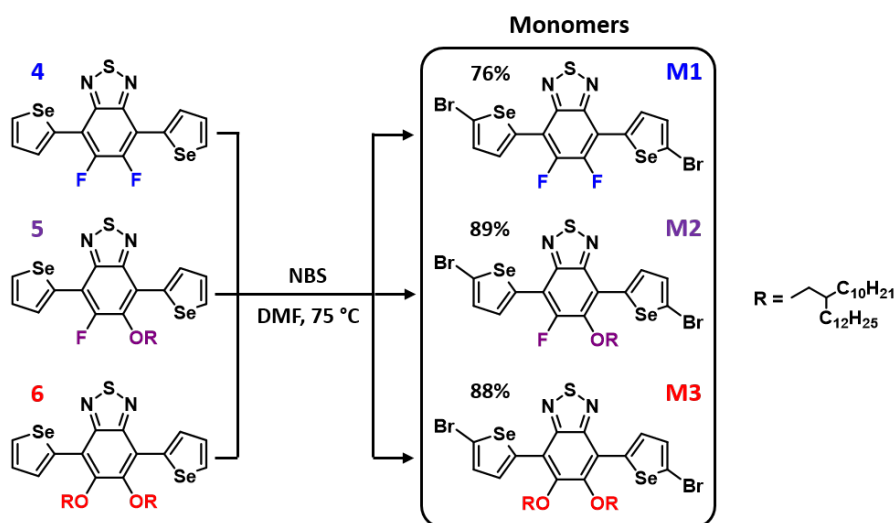
5,6-difluoro-4,7-di(selenophen-2-yl)benzo[c][1,2,5]thiadiazole (4), 5-((2-decyltetradecyl)oxy)-6-fluoro-4,7-di(selenophen-2-yl)benzo[c][1,2,5]thiadiazole (5) and 5,6-bis((2-decyltetradecyl)oxy)-4,7-di(selenophen-2-yl)benzo[c][1,2,5]thiadiazole (6):



In a microwave vial compound **1**, **2** or **3** (6 mmol) and tributyl(selenophen-2-yl)stannane (18 mmol) were dissolved in chlorobenzene (5 mL). Tetrakis(triphenylphosphine)palladium(0) (1 mol%) was added, and the resultant mixture was degassed for 30 min with argon and securely sealed. The vial was placed into a microwave reactor and heated at $100\text{ }^\circ\text{C}$ for 2 min, $110\text{ }^\circ\text{C}$ for 2 min and followed by $120\text{ }^\circ\text{C}$ for 2 hours. The crude mixture was filtrated over basic silica using hexane as an eluent and the solvent was removed under reduced pressure. Compound **4** and **5** were obtained as an orange solid after precipitation of crude product in MeOH. Compound **6** was afforded as a maroon syrup after purification of crude mixture by chromatography column using hexane/ethyl acetate 4:1. Compound **4** (2.2 g, 85%). ^1H NMR (400 MHz, CDCl_3) δ 8.51 (d, $J = 4.0$ Hz, 2H), 8.35 (d, $J = 5.6$ Hz, 2H), 7.52 (d, $J = 4$ Hz, 2H). ^{19}F NMR (376 MHz, CDCl_3) δ 116.3.

^{13}C NMR (100 MHz, CDCl_3) δ 149.6, 146.6, 136.6, 132.4, 130.0, 123.0, 114.9. Compound **5** (4.0 g, 87%). ^1H NMR (400 MHz, CDCl_3) δ 8.80 (dd, $J = 4.0, 0.8$ Hz, 1H), 8.50 (d, $J = 3.9$ Hz, 1H), 8.31 (d, $J = 5.7$ Hz, 1H), 8.25 (dd, $J = 5.7, 0.8$ Hz, 1H), 7.48 (m, 2H), 4.03 (d, $J = 6.3$ Hz, 2H), 2.04 (m, 1H), 1.55 (m, 2H), 1.22-1.5 (m, 38H), 0.88 (t, $J = 6.7$ Hz, 6H). ^{19}F NMR (376 MHz, CDCl_3) δ 117.4. ^{13}C NMR (100 MHz, CDCl_3) δ 153.4, 149.9, 149.6, 146.6, 136.5, 134.4, 132.5, 130.0, 129.7, 119.0, 113.2, 78.2, 39.1, 31.9, 31.0, 30.0, 29.7, 29.4, 26.3, 22.7, 14.1. Compound **6**. 5.4 g, 82%. ^1H NMR (400 MHz, CDCl_3) δ 8.53 (d, $J = 4.0$ Hz, 2H), 8.21 (d, $J = 5.6$ Hz, 2H), 7.45 (dd, $J = 5.7, 0.8$ Hz, 2H), 3.95 (d, $J = 6.4$ Hz, 4H), 1.98 (m, 2H), 1.43 (m, 4H), 1.22-1.40 (m, 76H), 0.89 (t, $J = 6.7$ Hz, 12H). ^{13}C NMR (100 MHz, CDCl_3) δ 152.6, 150.8, 138.5, 133.3, 132.7, 129.4, 119.3, 78.6, 39.1, 32.0, 31.2, 30.1, 29.8, 29.7, 29.4, 29.3, 27.4, 26.9, 22.7, 14.1.

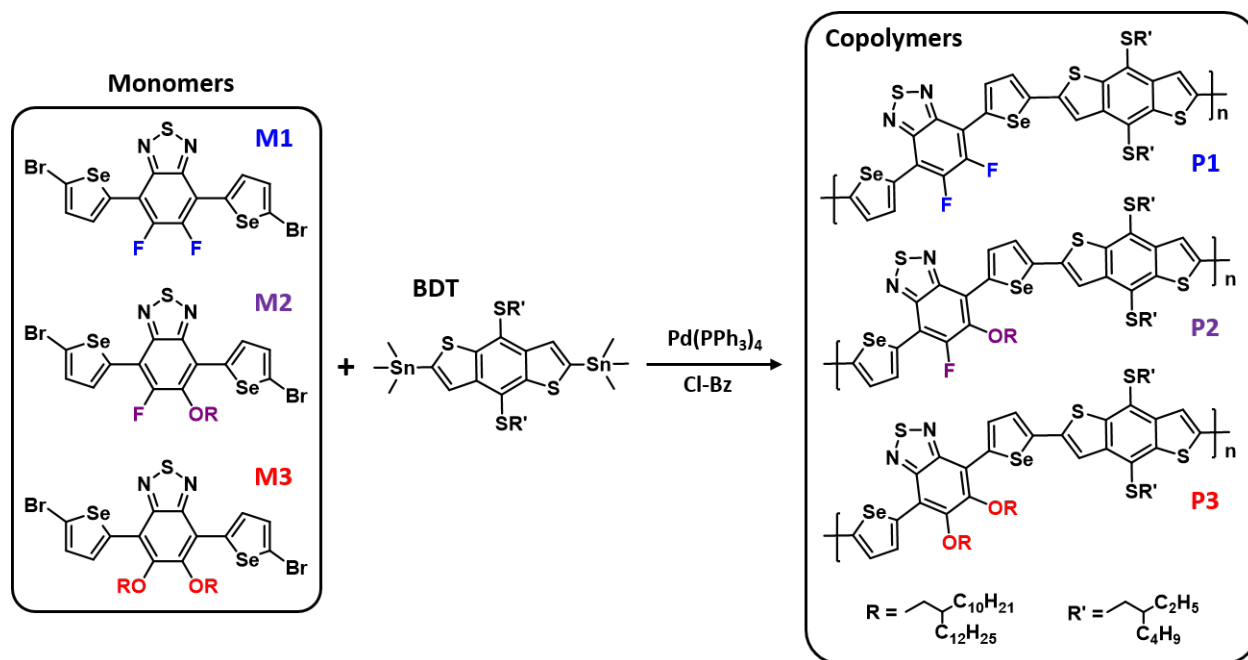
4,7-bis(5-bromoselenophen-2-yl)-5,6-difluorobenzo[c][1,2,5]thiadiazole (M1), **4,7-bis(5-bromoselenophen-2-yl)-5-((2-decyltetradecyl)oxy)-6-fluorobenzo[c][1,2,5]thiadiazole (M2)** and **4,7-bis(5-bromoselenophen-2-yl)-5,6-bis((2-decyltetradecyl)oxy)benzo[c][1,2,5]thiadiazole (M3)**



To a solution of **4**, **5** or **6** (3 mmol) in DMF (1 mL), NBS (9 mmol) was added. The mixture was stirred at 75 °C for 4 h. The mixture was then cooled to room temperature and water (100 mL) was added. The aqueous layer was extracted with diethyl ether (3 x 100 mL) and the organic layer was then washed with 5% NH_4Cl (3 x 100 mL), brine, water and then dried over Na_2SO_4 . Monomers **M1** and **M2** were obtained as a red solid after precipitation of crude product in MeOH. **M3** was

afforded as a red syrup after purification of crude mixture by chromatographic column using hexane/ethyl acetate 6:1. Monomer **M1**. 1.3 g, 76%. ^1H NMR (400 MHz, CDCl_3) δ 8.41 (d, $J = 4.0$ Hz, 2H), 7.34 (d, $J = 4$ Hz, 2H). ^{19}F NMR (376 MHz, CDCl_3) δ 118.1. ^{13}C NMR (100 MHz, CDCl_3) δ 149.3, 146.4, 136.6, 132.3, 129.6, 122.8, 114.2, 112.5. Monomer **M2**. 2.5 g, 89%. ^1H NMR (400 MHz) δ 8.58 (d, $J = 4.4$ Hz, 1H), 8.10 (d, $J = 4.4$ Hz, 1H), 7.38 (m, 2H), 4.00 (d, $J = 6.4$ Hz, 2H), 2.05 (m, 1H), 1.54 (m, 2H), 1.22-1.50 (m, 38H), 0.88 (t, $J = 6.7$ Hz, 6H). ^{19}F NMR (376 MHz, CDCl_3) δ 119.4. ^{13}C NMR (100 MHz, CDCl_3) δ 153.3, 149.2, 146.4, 139.3, 133.2, 132.3, 121.5, 112.7, 78.5, 39.1, 32.0, 30.9, 30.0, 29.8, 29.7, 29.4, 26.7, 22.7, 14.1. Monomer **M3**. 3.3 g, 88%. ^1H NMR (400 MHz, CDCl_3) δ 8.39 (d, $J = 4.4$ Hz, 2H), 7.36 (d, $J = 4.4$ Hz, 2H), 3.98 (d, $J = 6.4$ Hz, 4H), 2.00 (m, 2H), 1.44 (m, 4H), 1.22-1.40 (m, 76H), 0.88 (t, $J = 6.7$ Hz, 12H). ^{13}C NMR (100 MHz, CDCl_3) δ 152.2, 150.2, 140.25, 132.8, 132.7, 120.0, 119.6, 78.9, 39.0, 32.0, 31.2, 30.1, 29.8, 29.7, 29.4, 27.4, 26.8, 22.7, 14.1.

General procedure for the Synthesis of copolymers P1-P3



In a microwave vial compound (4,8-bis(2-ethylhexyl)thio)benzo[1,2-b:4,5-b']dithiophene-2,6-diyl)bis(trimethylstannane) (0.30 mmol) and equimolar amount of **M1**, **M2** or **M3** were dissolved in anhydrous chlorobenzene (0.5 mL) followed by addition of tetrakis(triphenylphosphine)palladium(0) (2 mol%), the resultant mixture was degassed for 30 min with argon and securely sealed. The glass vial was placed into a microwave reactor and heated at

140 °C for 2 min, 160 °C for 2 min, and followed by 180 °C for 30 min. After being cooled to room temperature, the reaction mixture was precipitated into a mixture of methanol (200 mL) and concentrated HCl (2 mL) and stirred for 1 h at RT. The precipitate was filtered and extracted (Soxhlet) with methanol, acetone, n-hexane and chloroform. The remaining polymer was dissolved in chlorobenzene and precipitated into methanol, filtered, and dried under vacuum to achieve the desired polymers as a dark blue solid. The ^1H NMR spectrum for **P1** was very broad with no detectable peaks, while polymers **P2** and **P3** exhibited considerable broadening of the aromatic and methylene peaks and only alkyl sidechain protons were fully observable. We attribute this to the aggregation effects. **P1**: Yield 95 mg, GPC: $M_n = 21,300$ g/mol, $D = 1.9$; UV-Vis: $\lambda_{max} = 574$ nm (dilute chlorobenzene solution). **P2**: Yield 92 mg, ^1H NMR (400 MHz, CDCl_3) δ 4.22 (4H), 3.02 (4H), 1.10-1.80 (71H), 0.87 (6H); GPC: $M_n = 34,700$ g/mol, $D = 2.0$; UV-Vis: $\lambda_{max} = 607$ nm (dilute chlorobenzene solution). **P3**: Yield 95 mg, ^1H NMR (400 MHz, CDCl_3) δ 8.64 (2H), 7.84 (2H), 4.09 (4H), 3.05 (4H), 1.10-1.80 (114H), 0.87 (12H); GPC: $M_n = 37,200$ g/mol, $D = 2.0$ UV-Vis: $\lambda_{max} = 577$ nm (dilute chlorobenzene solution).

NMR characterization

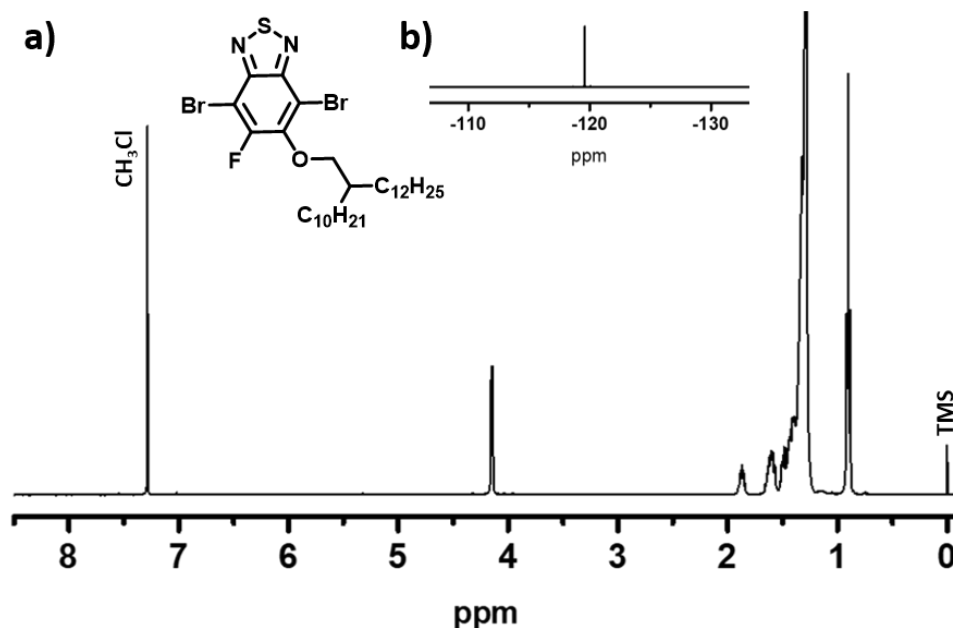


Figure S1. a) ^1H and b) ^{19}F NMR spectrum of **2**.

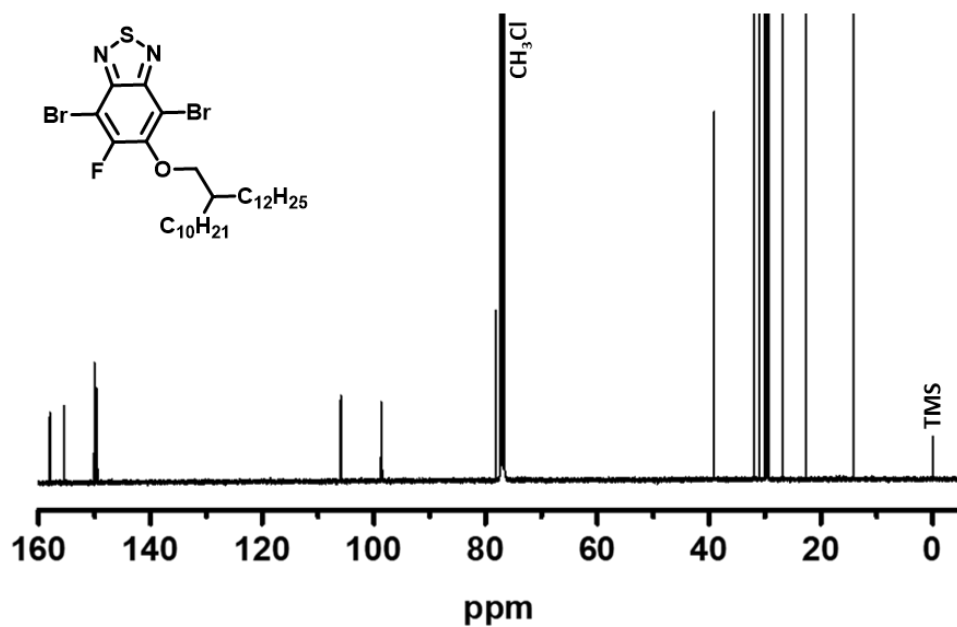


Figure S2. ^{13}C NMR spectrum of **2**.

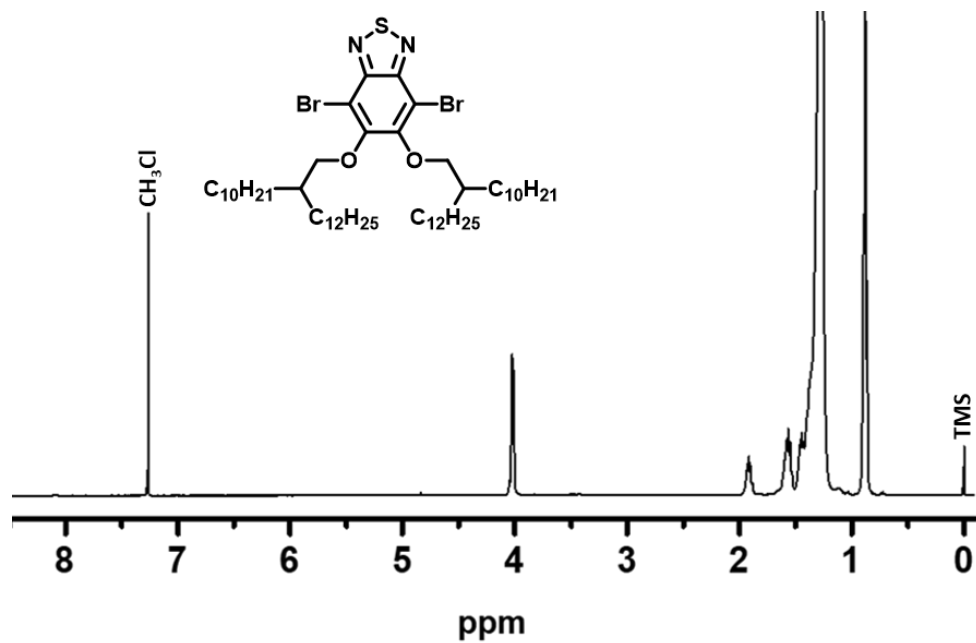


Figure S3. ^1H NMR spectrum of **3**.

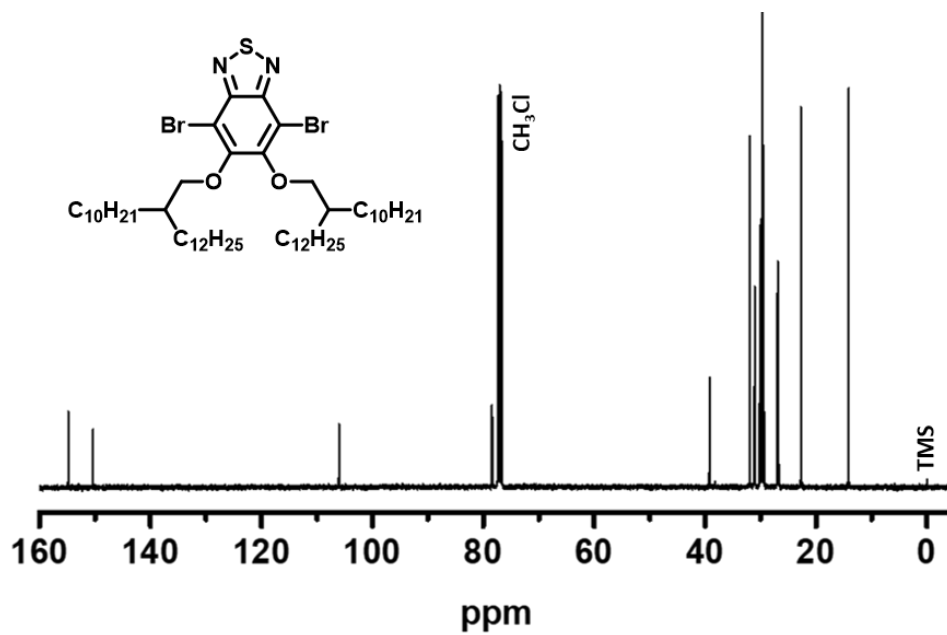


Figure S4. ^{13}C NMR spectrum of **3**.

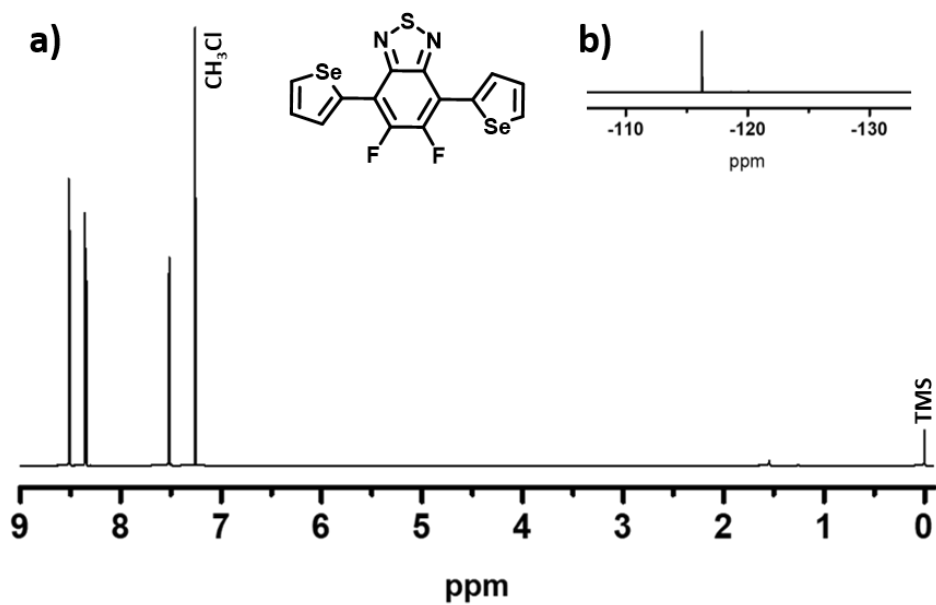


Figure S5. a) ^1H and b) ^{19}F NMR spectrum of **4**.

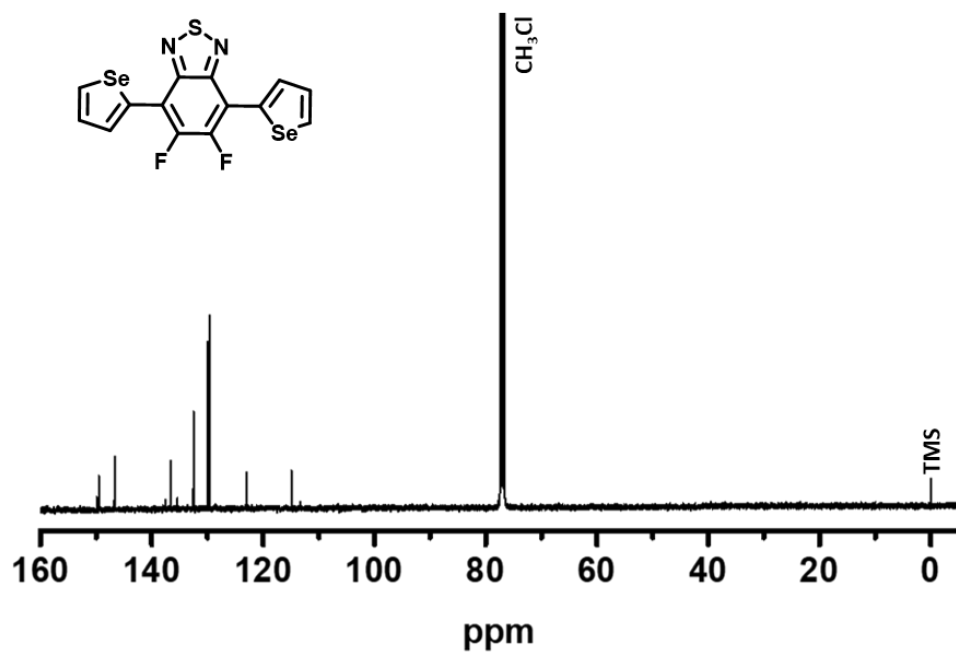


Figure S6. ^{13}C NMR spectrum of **4**.

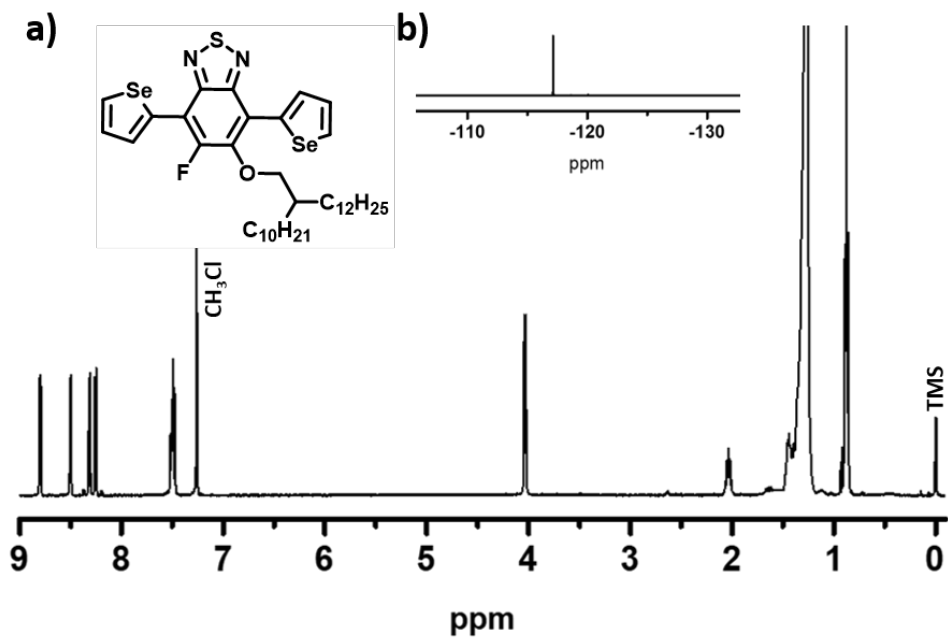


Figure S7. a) ^1H and b) ^{19}F NMR spectrum of **5**.

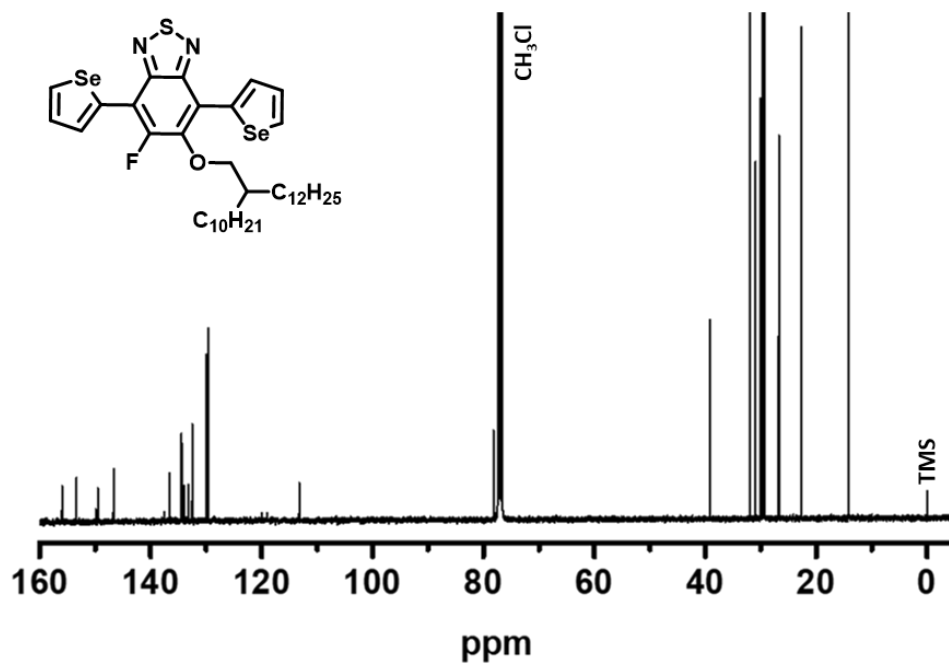


Figure S8. ^{13}C NMR spectrum of **5**.

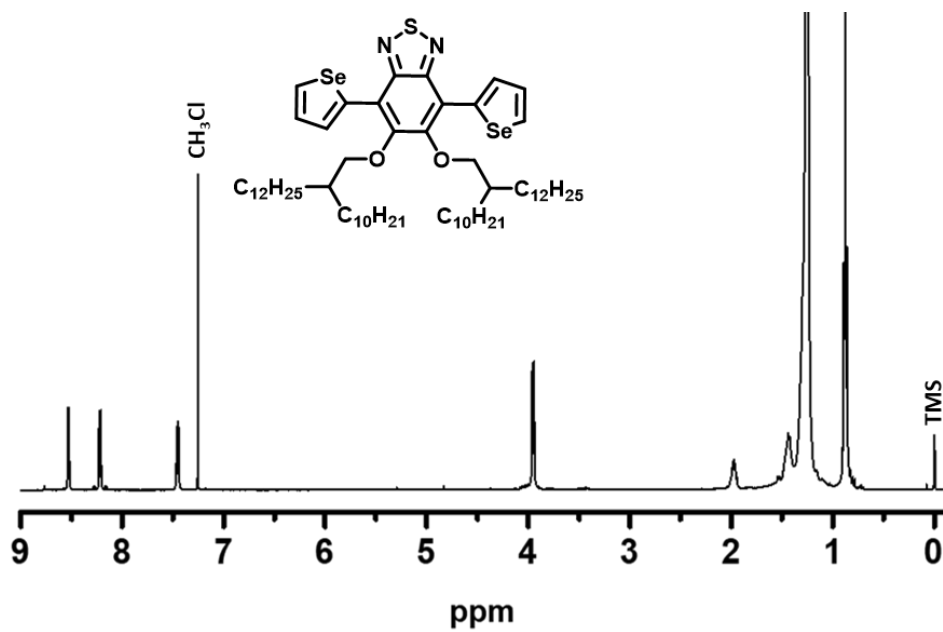
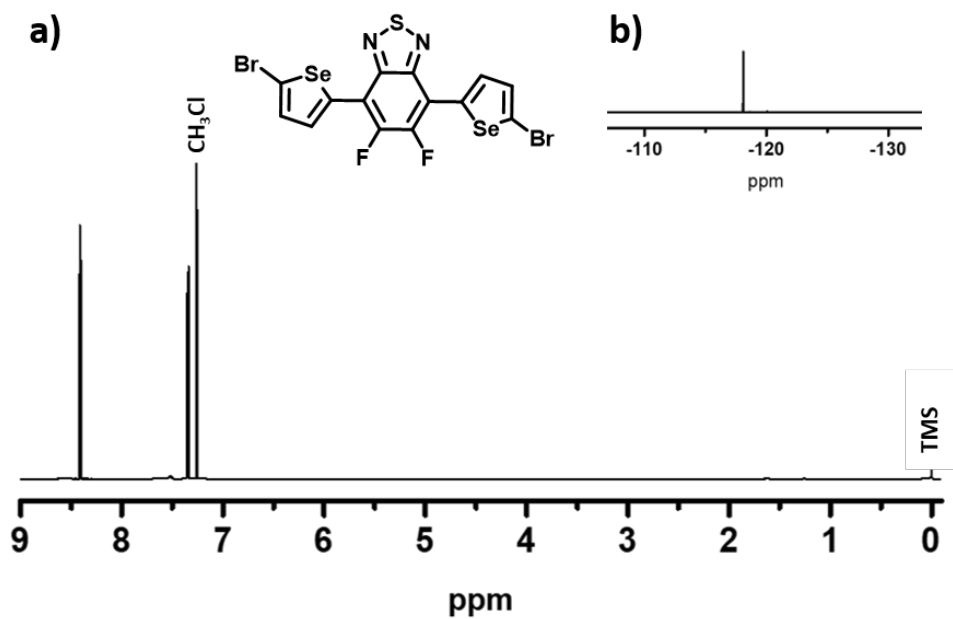
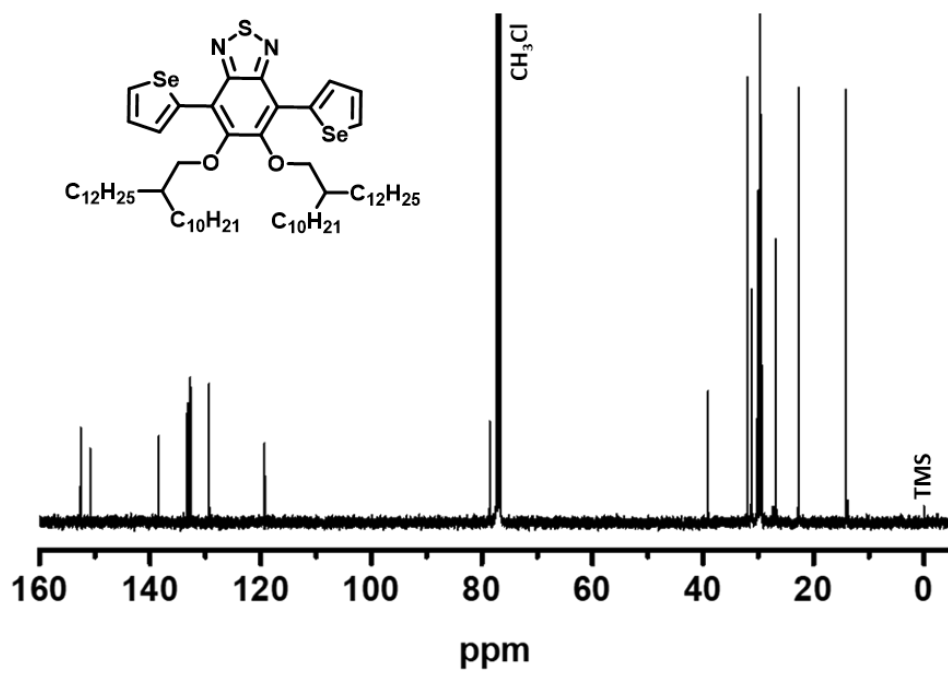


Figure S9. ^1H NMR spectrum of **6**.



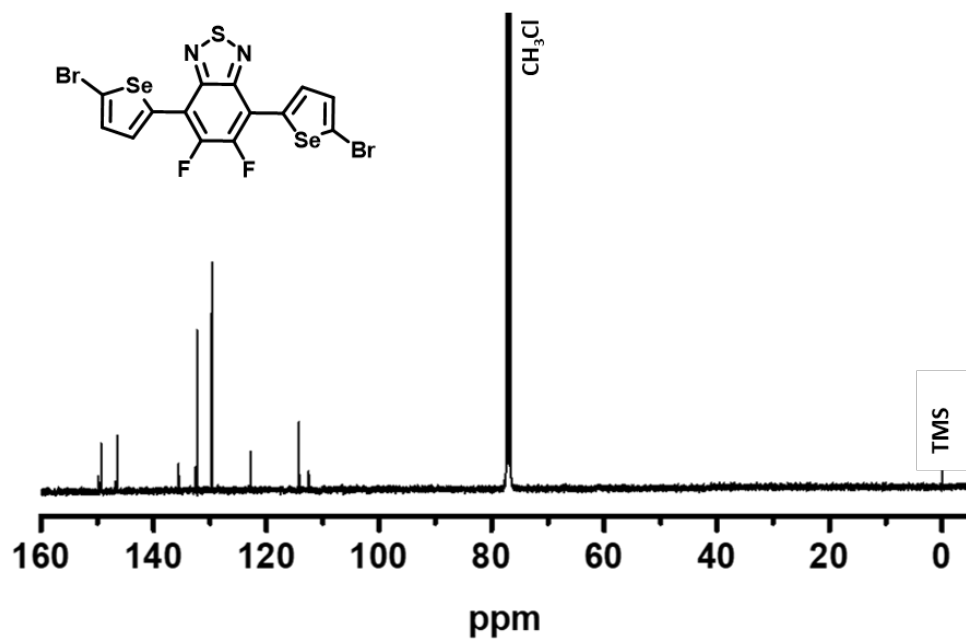


Figure S12. ^{13}C NMR spectrum of **M1**.

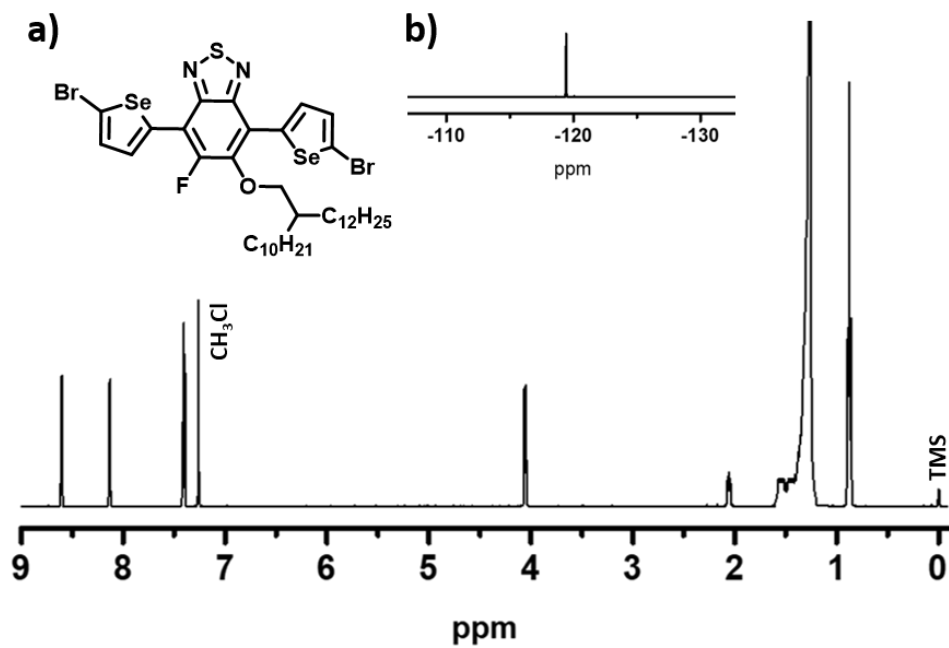


Figure S13. a) ^1H and b) ^{19}F NMR spectrum of **M2**.

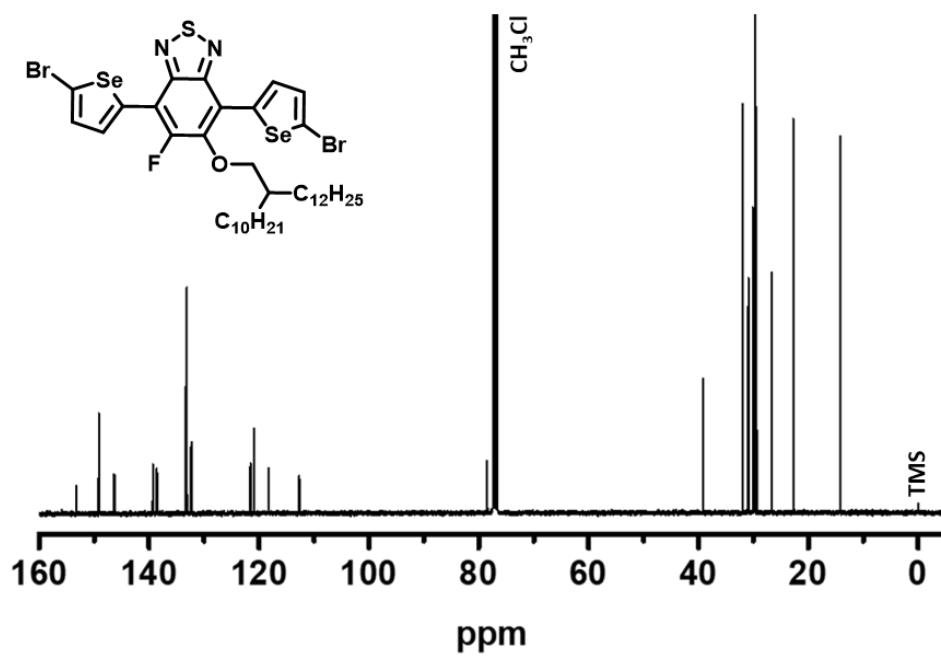


Figure S14. ^{13}C NMR spectrum of **M2**.

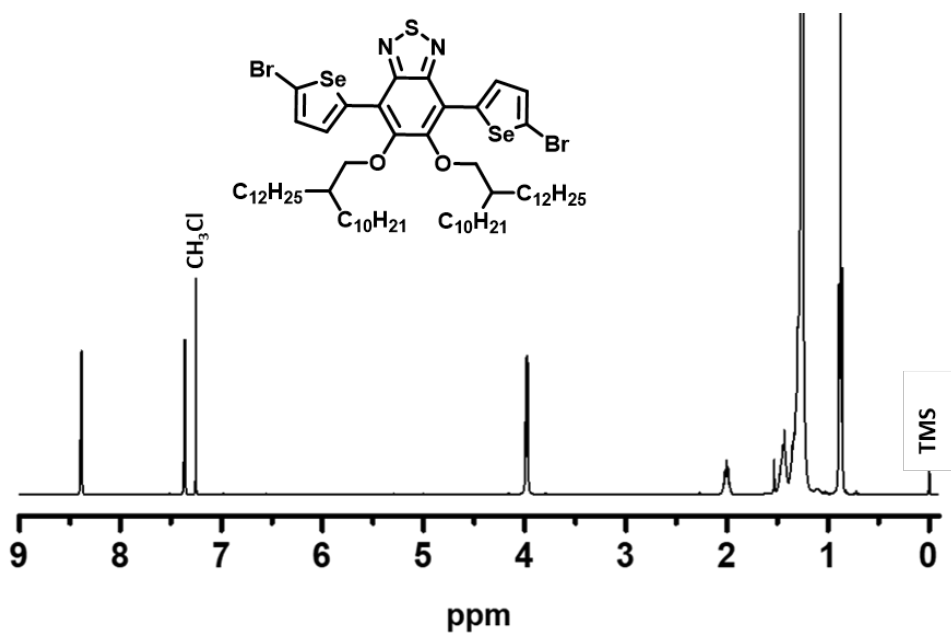


Figure S15. ^1H NMR spectrum of **M3**.

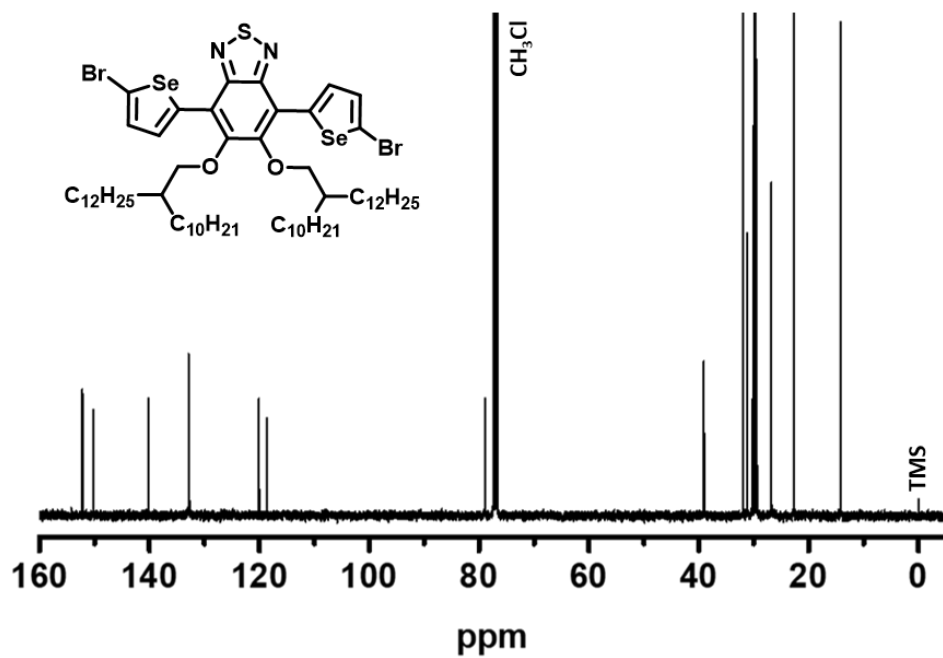


Figure S16. ^{13}C NMR spectrum of **M3**.

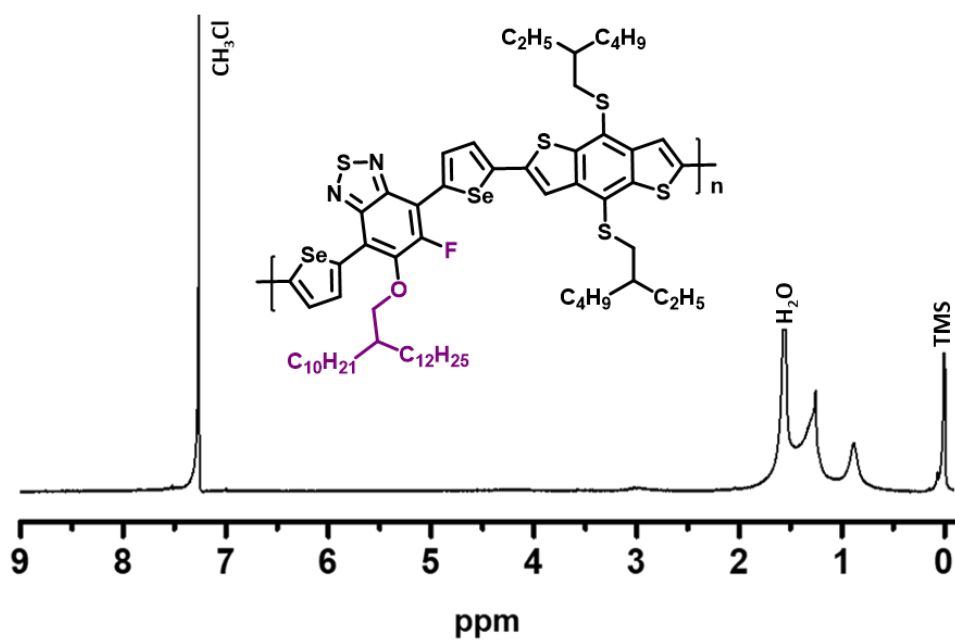


Figure S17. ^1H NMR spectrum of **P2**.

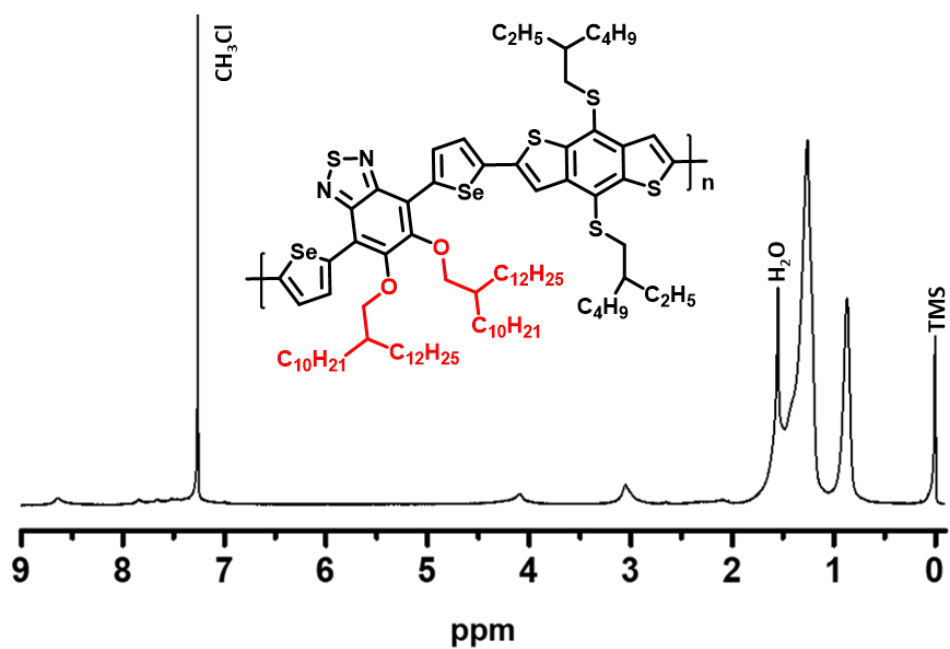


Figure S18. ^1H NMR spectrum of **P3**.

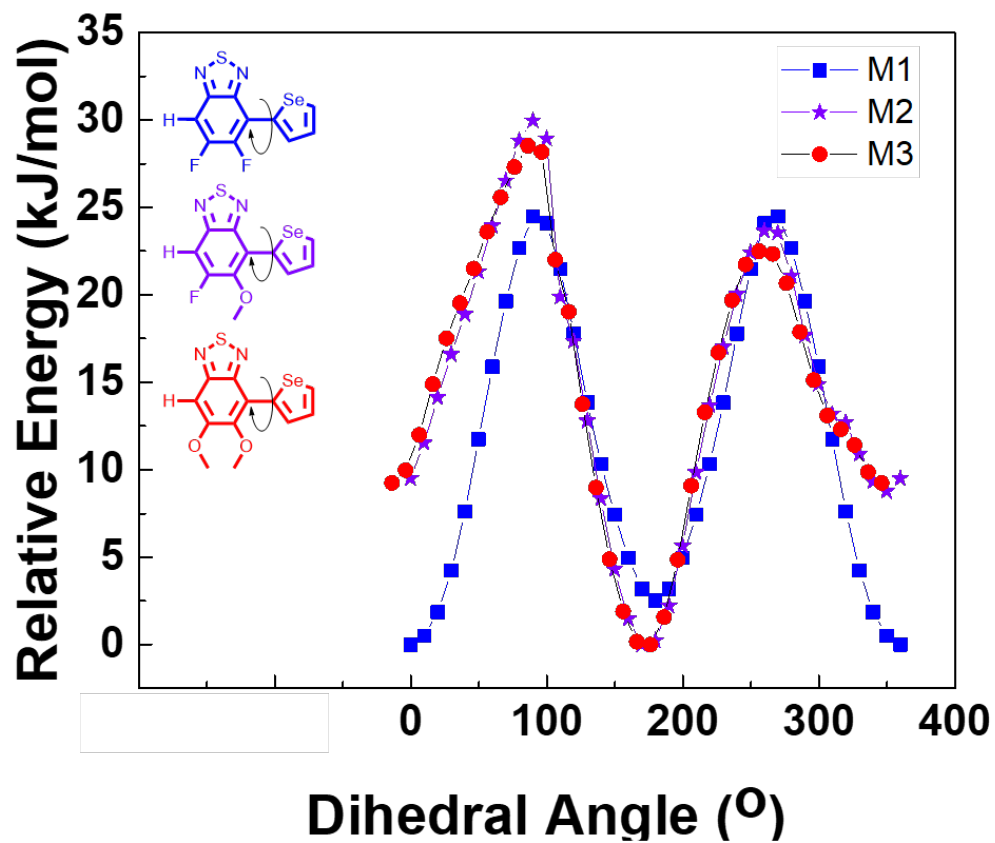


Figure S19. B3LYP-D3/6-31G(d,p) calculated potential energy scan of dihedral angles contained in monomers **M1-M3**.

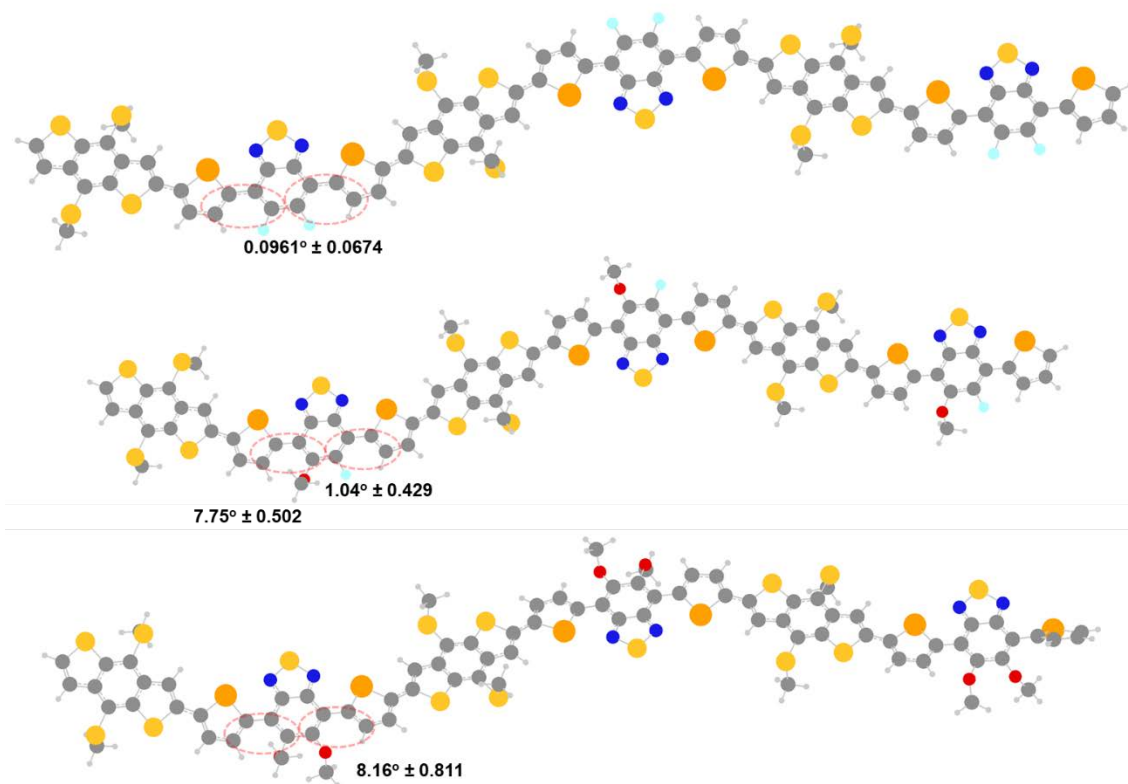


Figure S20. B3LYP-D3/6-31G(d,p) calculated optimized geometries of **P1** (top), **P2** (middle), and **P3** (bottom). Dihedral angles of interest are indicated with dashed ovals. The branched alkyl chains are truncated to methyl (-CH₃) caps to reduce computation cost. Colour code: yellow = sulfur, blue = nitrogen, grey = carbon, white = hydrogen, red = oxygen, cyan = fluorine, and orange = selenium.

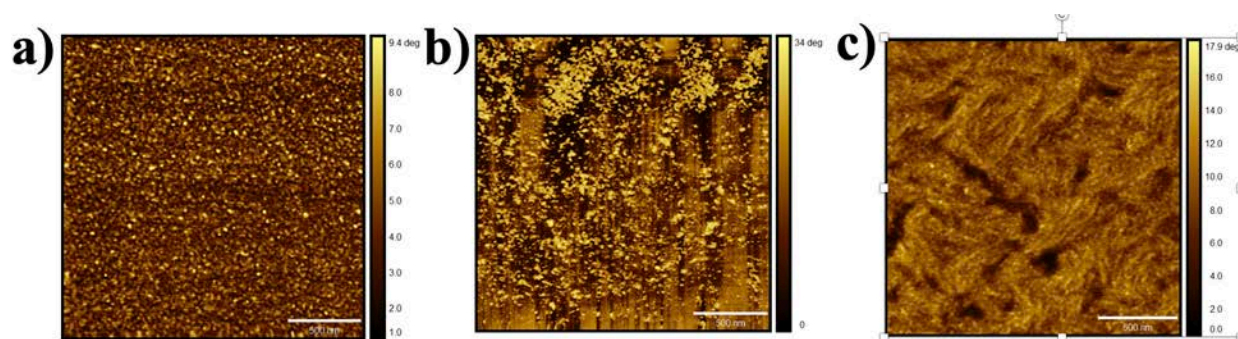


Figure S21. Atomic force microscopy (AFM) phase images of a) **P1**; b) **P2**, and c) **P3** in thin films. Scale bar = 500 nm.

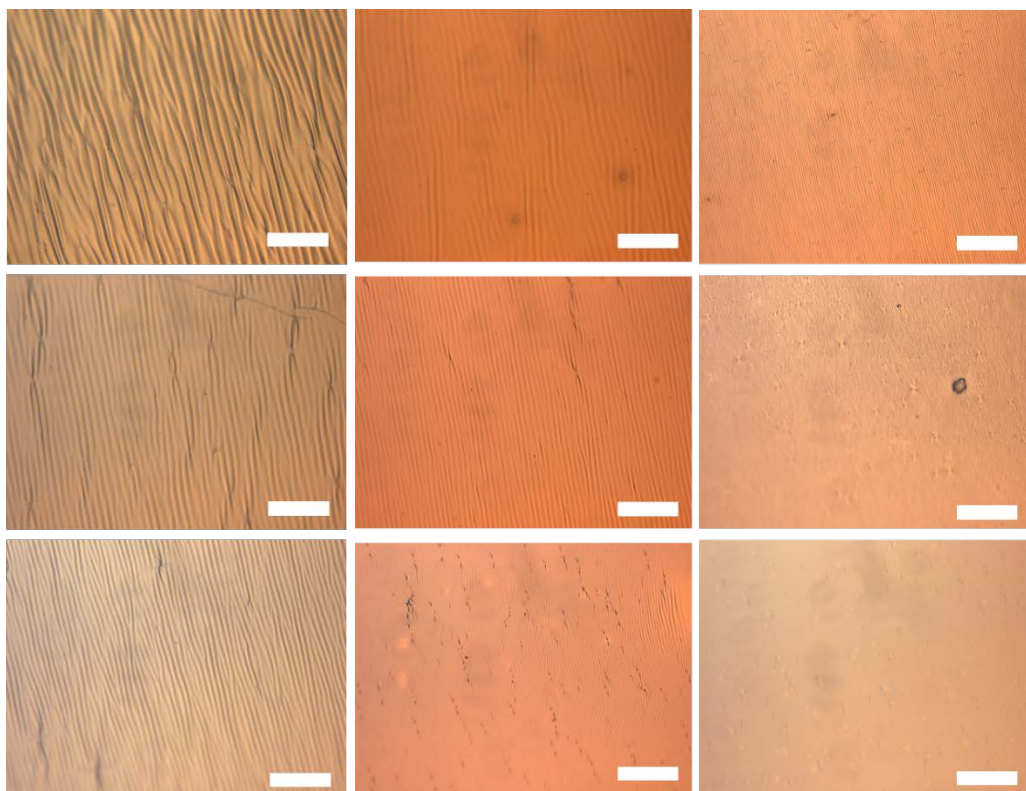


Figure S22. Representative buckled films of **P1** (left), **P2** (middle), and **P3** (right) on PDMS slabs visualized through optical microscope. Images taken from polymers spincoated at 500 RPM (top), 1000 RPM (middle), and 1500 RPM (bottom) to produce films of varying thicknesses. Scale bar = 25 μm .

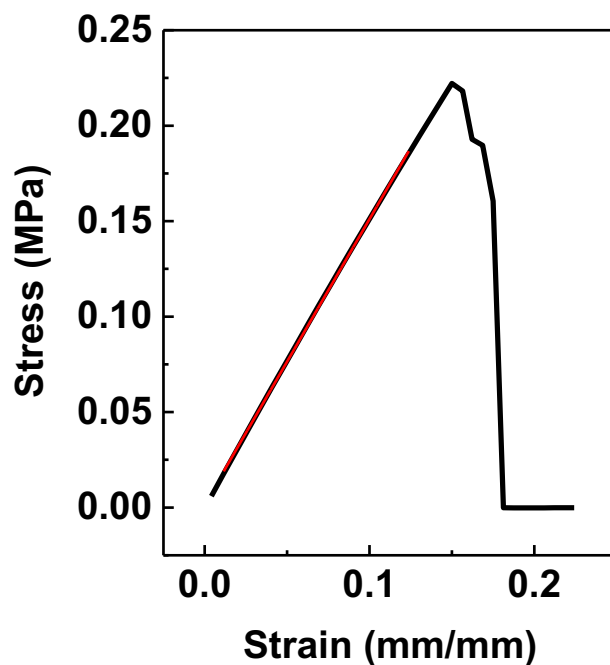


Figure S23. Stress-strain curve of 10:1 PDMS (base:crosslinker) used in the buckling metrology. The linear region of the elastic regime was used to calculate the elastic modulus, and this value was then used to measure the elastic modulus of conjugated polymer thin films of **P1** to **P3**.

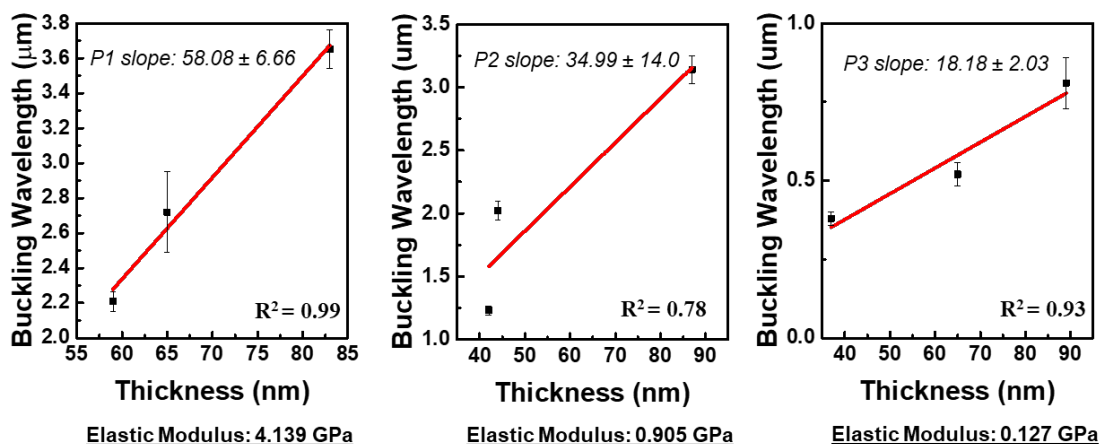


Figure S24. Buckling wavelength vs conjugated polymer thin film thickness of films of **P1** (left), **P2** (middle) and **P3** (right).

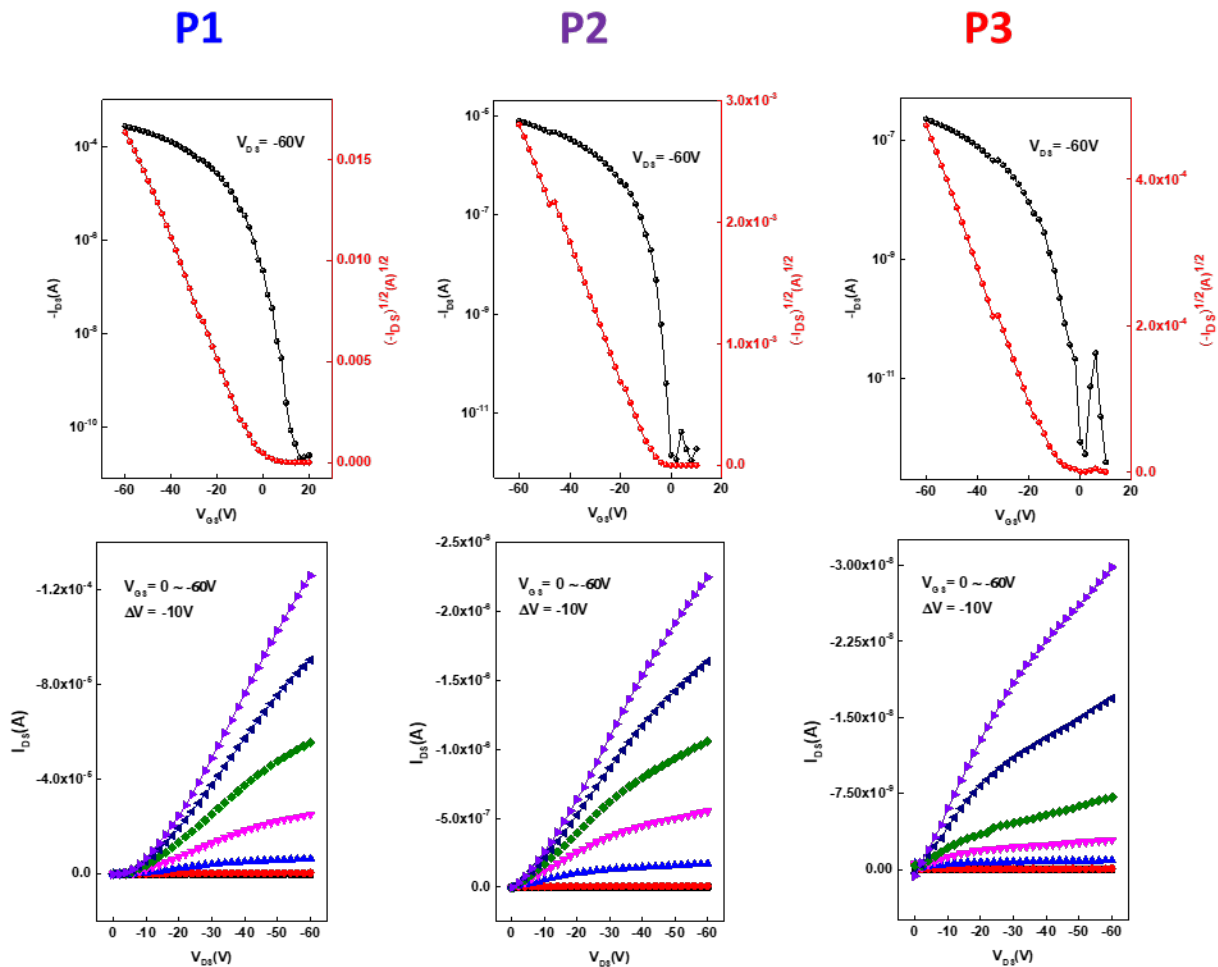


Figure S25. Typical transfer (top) and output (bottom) curves of polymers **P1-P3** measured at a source-drain voltage of -60V for the transfers curves, and at gate-source voltage intervals of -10V for the output curves.

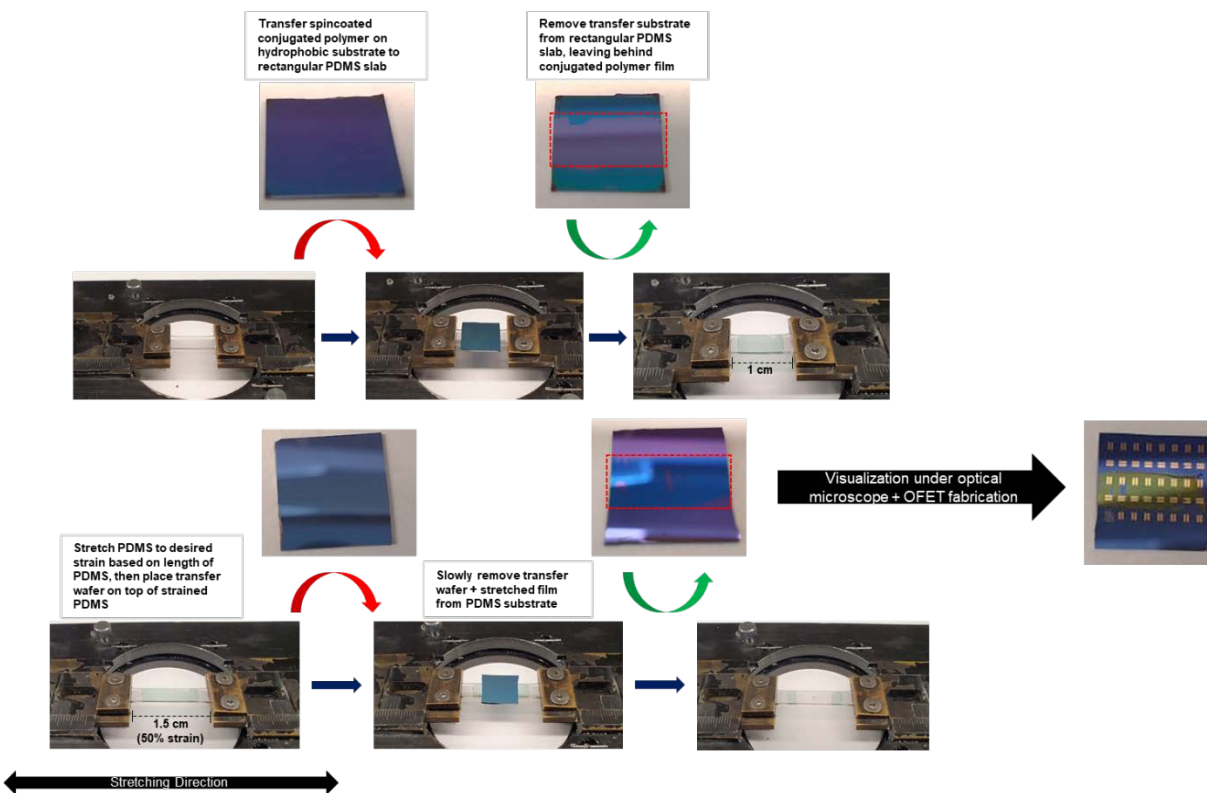


Figure S26. Stepwise image of the transfer process used for measuring crack-onset strain and organic field-effect transistor fabrication of transferred and strained films. The sample process stretches a conjugated polymer to 50% strain before being transferred to a silicon receiving wafer. Films are then subjected to optical microscopy and then 50 nm gold source and drain electrodes oriented parallel and perpendicular to the applied strain direction are evaporated on top to complete the device. Devices are subsequently brought into a N_2 -filled glovebox for testing.

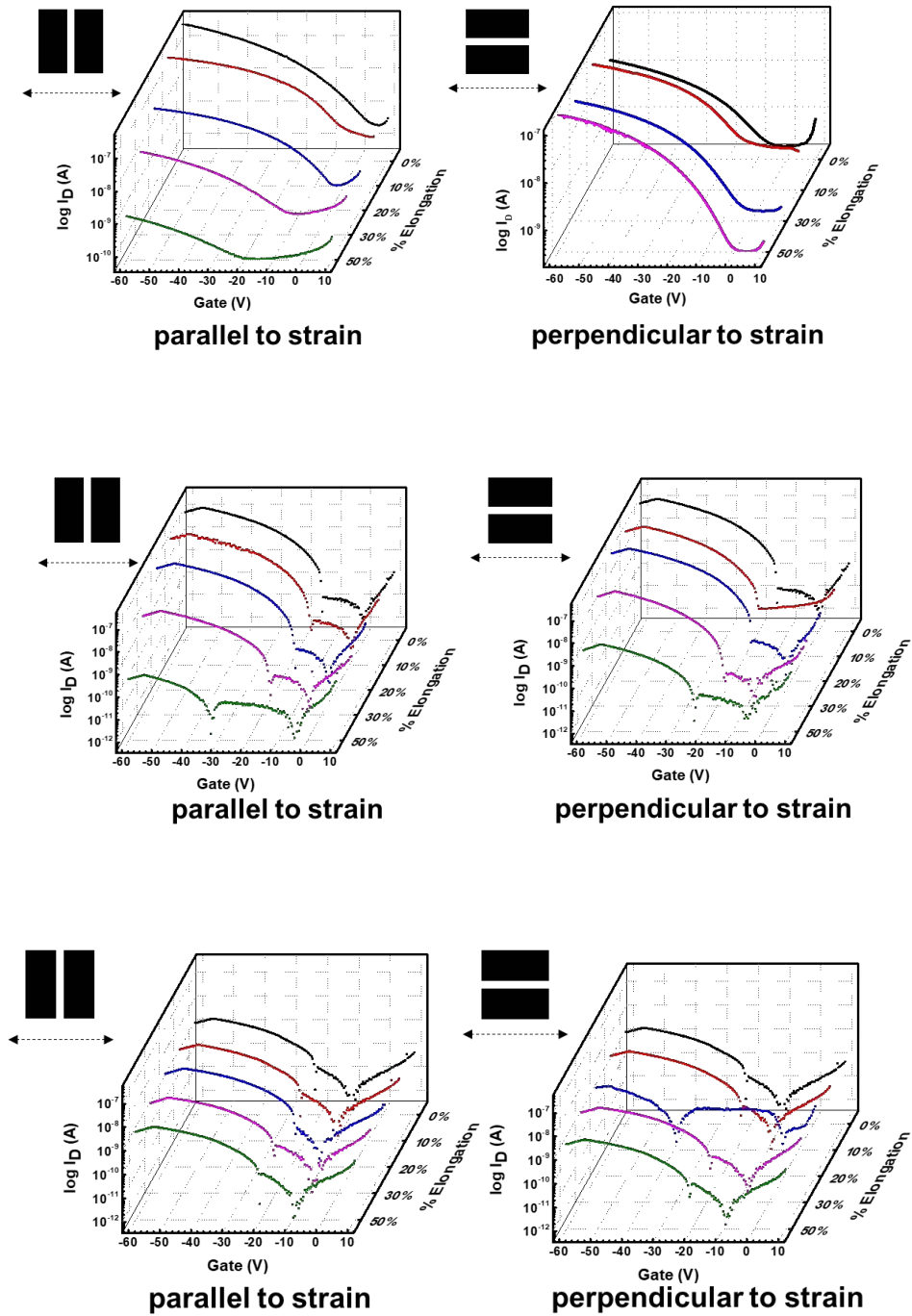


Figure S27. Transfer curves of **P1** (top), **P2** (middle), and **P3** (bottom) at 0, 10, 20 and 30% strain. $V_{D_S} = -60$ V. Linear fitting was conducted in the saturation regime.

Table S1. Average hole mobility (μ_{ave}), mobility retention (%), threshold voltage (V_{th}), and $I_{\text{ON/OFF}}$ current ratios for OFETs fabricated from **P1-P3** at strains ranging from 0-30%. Results are averaged from at least 5 devices.

| Strain (%) | / \perp | P1 | | | | P2 | | | | P3 | | | |
|------------|-----------|--|---------------------|---------------------|---------------------|--|---------------------|---------------------|---------------------|--|---------------------|---------------------|---------------------|
| | | μ_{ave} ($\times 10^{-3}$ cm ² /Vs) | μ Retention (%) | V_{th} (V) | $I_{\text{ON/OFF}}$ | μ_{ave} ($\times 10^{-3}$ cm ² /Vs) | μ Retention (%) | V_{th} (V) | $I_{\text{ON/OFF}}$ | μ_{ave} ($\times 10^{-3}$ cm ² /Vs) | μ Retention (%) | V_{th} (V) | $I_{\text{ON/OFF}}$ |
| 0 | | 7.01 \pm 1.93 | N/A | -5.53 | 10 ³ | 2.334 \pm 0.421 | N/A | -18.5 | 10 ³ | 0.0669 \pm 0.00649 | N/A | -12.2 | 10 ³ |
| 10 | | 0.224 \pm 0.203 | 3.2 | -6.31 | 10 ² | 0.827 \pm 0.569 | 35 | -10.1 | 10 ³ | 0.0263 \pm 0.00787 | 39 | -13.8 | 10 ³ |
| | \perp | 4.55 \pm 1.68 | 65 | -8.77 | 10 ² | 3.76 \pm 0.155 | 100 | -20.4 | 10 ³ | 0.0347 \pm 0.00528 | 52 | -14.6 | 10 ³ |
| 20 | | 0.126 \pm 0.110 | 2.4 | -5.16 | 10 ² | 0.613 \pm 0.578 | 26 | -17.8 | 10 ³ | 0.0348 \pm 0.00510 | 52 | -11.4 | 10 ³ |
| | \perp | 0.172 \pm 0.0531 | 11.6 | -8.22 | 10 ² | 2.116 \pm 0.231 | 91 | -19.6 | 10 ³ | 0.0231 \pm 0.0154 | 35 | -13.4 | 10 ³ |
| 30 | | 0.169 \pm 0.0859 | 1.8 | -8.07 | 10 ² | 0.204 \pm 0.0637 | 8.7 | -15.7 | 10 ³ | 0.0328 \pm 0.00394 | 49 | -11.5 | 10 ³ |
| | \perp | 0.127 \pm 0.101 | 10.8 | -7.18 | 10 ² | 0.576 \pm 0.000167 | 25 | -19.9 | 10 ³ | 0.0237 \pm 0.00549 | 35 | -12.5 | 10 ³ |

References

- 1 A. A. B. Alghamdi, D. C. Watters, H. Yi, S. Al-Faifi, M. S. Almeataq, D. Coles, J. Kingsley, D. G. Lidzey and A. Iraqi, Selenophene vs. thiophene in benzothiadiazole-based low energy gap donor–acceptor polymers for photovoltaic applications, *J. Mater. Chem. A*, 2013, **1**, 5165–5171.
- 2 J.-L. Wang, K.-K. Liu, S. Liu, F. Xiao, Z.-F. Chang, Y.-Q. Zheng, J.-H. Dou, R.-B. Zhang, H.-B. Wu, J. Pei and Y. Cao, Donor End-Capped Hexafluorinated Oligomers for Organic Solar Cells with 9.3% Efficiency by Engineering the Position of π -Bridge and Sequence of Two-Step Annealing, *Chem. Mater.*, 2017, **29**, 1036–1046.